

Anomalous thermal dynamics of Bragg gratings inscribed in germanosilicate optical fiber

A. RAHMAN*, K. VENU MADHAV, B. SRINIVASAN^a, S. ASOKAN

Department of Instrumentation, Indian Institute of Science, Bangalore 560012, India

^aDepartment of Electrical Engineering, Indian Institute of Technology, Madras 600036, India

An interesting, periodic appearance of a new peak has been observed in the reflected spectrum of a Fiber Bragg Grating (FBG) inscribed in a germanosilicate fiber during thermal treatment. The new peak occurs on the longer wavelength side of the spectrum during heating and on the shorter wavelength side during cooling, following an identical reverse dynamics. Comparison with a commercial grating with 99.9% reflectivity shows a similar decay dynamics. It is proposed that the distortion due to simultaneous erasure and thermal expansion of the index modulation profile may be responsible for the observed anomaly. The reported results help us in understanding the thermal behavior of FBGs and provide additional insights into the mechanisms responsible for the photosensitivity in germanosilicate fibers.

(Received November 21, 2008; accepted January 21, 2009)

Keywords: Fiber Bragg gratings, Thermal erasure, Degradation dynamics

1. Introduction

Fiber Bragg Gratings (FBGs) have become one of the most popular optical devices that use the phenomenon of ultraviolet (UV) photosensitivity in germanosilicate fibers. The formation of a grating in the core of an optical fiber was first demonstrated by Hill et al [1] and with the impressive progress in the fabrication techniques [2], FBGs have emerged as an ideal candidate for applications in different fields such as optical telecommunications [3], optical fiber based sensors [4], etc.

Studies on thermal stability of FBGs are necessary and important in order to predict their suitability in practical scenarios. In literature, there are extensive reports on the thermal degradation characteristics of FBGs in various fibers. For example, Erdogan *et al* [5] have proposed a ‘power law’ model for thermal decay of UV induced index change in a germanosilicate fiber; carriers excited during inscription are trapped in a broad distribution of trap states and the rate of thermal degradation has been found to depend on the trap depth. Further studies [6-11] have shown that the decay of gratings written in different fibers also follow the ‘power law’ model described by Erdogan et al but with different coefficients. It is also interesting to note that there is some disagreement [7,9] in the thermal stability analysis of gratings written in hydrogen loaded and non-hydrogen loaded fibers. Although the thermal decay of boron co-doped germanosilicate fiber shows a ‘power law’ dependency, hydrogen loading modifies it to a ‘log-time’ behavior [12].

In this paper, we present a study on the thermal erasure dynamics of fiber Bragg gratings inscribed in non-hydrogenated germanosilicate fibers. Since any changes in the index modulation profile of the grating manifests itself as a distortion in the reflections/transmission spectrum, the

thermal erasure dynamics of a grating can be deciphered by observing the grating spectra.

First, the experimental details are described. Subsequently, the results which bring out the anomalous thermal dynamics & its origin are discerned through a series of specific experiments are described. Lastly, an analysis of the results and a summary of the thermal decay process of Fiber Bragg Gratings are presented.

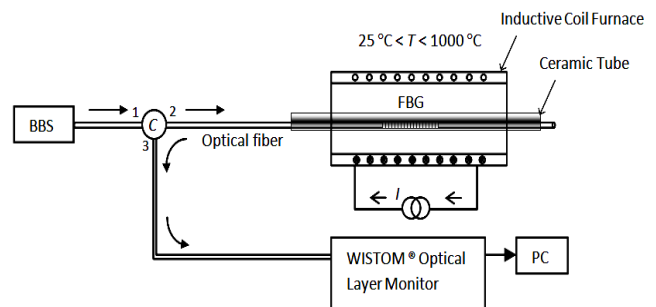


Fig. 1. Experimental layout for thermal erasure of fiber Bragg grating. C: Circulator. BBS: Broadband source.

2. Experimental details

The phase-mask technique was used to inscribe gratings in a germano-silicate fiber. Photosensitive fiber (Nufern GF), with 5.5 mol % germania concentration (NA=0.13) was placed in close proximity of a Bragg Photonics phase-mask with a period $\Lambda_{pm} = 1054.7$ nm. A Braggstar Industrial LN KrF excimer laser (248nm, UV) with a pulse energy of 2.56mJ at 200Hz having a spatial coherence of 1.5mm along the fiber axis, was used to inscribe a 3mm long grating in about 7 min at a Bragg wavelength $\lambda_B^1 = 1527.2$ nm.

It is found that the grating growth dynamics follows the typical ‘power law’ profile with an exponent of 0.5. After inscription, the grating is inserted into a ceramic tube which is then placed axially at the center of a cylindrical Inductive Coil Furnace (ICF) as shown in Fig.1. The furnace temperature, T , is ramped up/down in the range $25^\circ\text{C} < T < 1000^\circ\text{C}$ by controlling the current (I) flowing through the coils. A Super Luminescent Diode (SLD) broadband source (C-Band: 1524nm-1572nm) connected to port-1 of a 3-port fiber optic circulator is used to launch light into the grating-inscribed fiber connected to port-2 of the circulator. The light reflected from the grating is redirected into a WISTOM Optical Layer Monitor (OLM) via port-3.

The reflection spectrum of the grating shown in Fig.2 reveals side-lobes, on the shorter wavelength side of the Bragg resonance peak. The observed spectral shape is attributed to the gradually increasing/decreasing decoupling coefficient (κ_{dc}) arising due to the non-uniform intensity profile of the UV laser along the fiber axis.

Fig.3 shows the intensity distribution of the excimer laser spot profiled by scanning a narrow vertical (y -axis) slit along the fiber axis (x -axis). Here, a Newport power meter (Model 918) has been used to measure the intensity at discrete points along x -axis. This non-uniform laser intensity profile causes the observed index profile (side lobes) of the inscribed grating. Simulation (MATLAB) of the reflected spectrum using the measured intensity profile of the laser has shown a good agreement with the observed reflection spectrum.

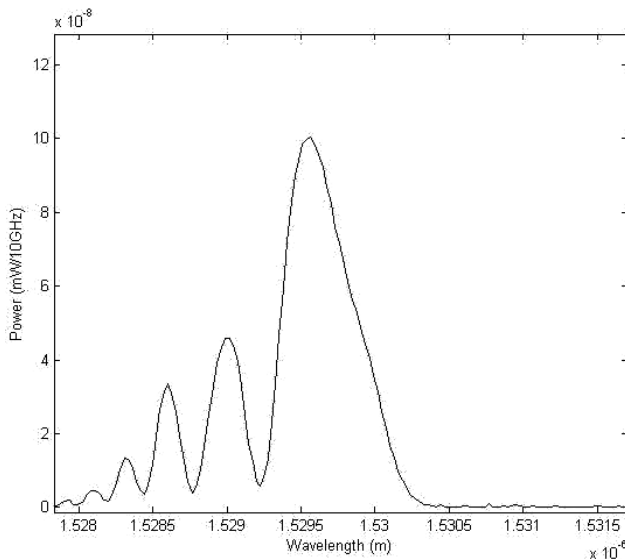


Fig.2. Reflection spectrum of the grating at 35 °C.

In the present study, experiments are conducted in two categories: first the thermal erasure dynamics of gratings inscribed in the laboratory in fibers with germanium and boron co-doping having side lobes and commercial gratings without side-lobes have been studied. In the

second category, the effect of cladding, thermal-expansion/thermo-optic coefficients, heating and cooling cycles are analyzed.

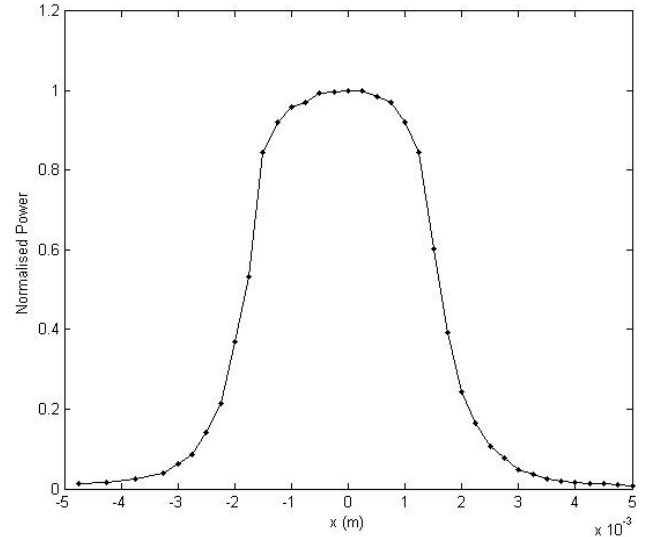


Fig.3. Laser intensity profile along the fiber (x -axis).

3. Thermal erasure dynamics of fiber Bragg gratings

3.1 Anomalous dynamics

As mentioned earlier, the Bragg grating at $\lambda_B^1 = 1527.2\text{nm}$ is inscribed in a germanium doped (5.5 mol%) silica fiber and thermally treated in the temperature range $26^\circ\text{C} < T < 900^\circ\text{C}$ over a span of 12 hrs in ICF. The grating has been annealed for 30min at every 100°C and the reflection spectrum is recorded at 10°C intervals.

It is most interesting to note that an anomalous Bragg peak has been observed in the present experiments, at λ_{Bn}^1 , adjacent to the main Bragg peak ($\lambda_B^1 < \lambda_{Bn}^1$) in the temperature range $65^\circ\text{C} < T < 125^\circ\text{C}$. With increase in temperature (65°C to 125°C), a decrease in reflected power is observed at λ_B^1 with simultaneous increase in reflected power at λ_{Bn}^1 . It is also interesting to note that this cycle of appearance and growth of a new Bragg peak at the longer wavelength side with the simultaneous disappearance of the old peak repeats periodically in the temperature range $125^\circ\text{C} < T < 700^\circ\text{C}$.

Fig. 4 (a-f) shows the growth dynamics of the Bragg peaks for a representative thermal window $125^\circ\text{C} < T < 175^\circ\text{C}$. The appearance & growth of λ_{Bn}^1 and the simultaneous progressive disappearance of λ_B^1 is clearly seen in successive plots (a), (b), (c), (d), (e) and (f) in Fig. 4.

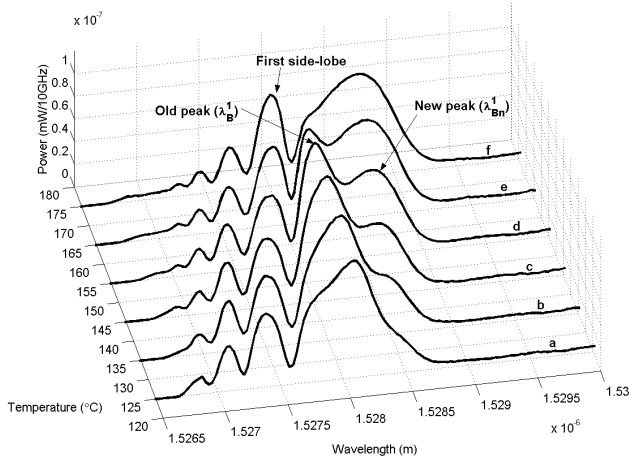


Fig. 4. Growth of new FBG reflection peak λ_{Bn}^1 with an increase in temperature. Plots (a)-(f) represent the FBG reflection spectrum for a representative thermal window $125^\circ\text{C} < T < 175^\circ\text{C}$.

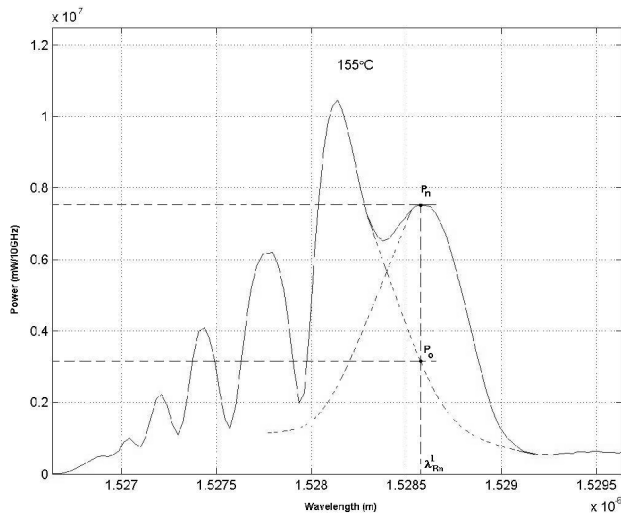


Fig. 5. Power levels P_o and P_n of the two reflection peaks at λ_{Bn}^1 , at a temperature of 155°C . The dotted curve represents the grating reflection spectra in the absence of the new peak.

In the present experiments, the evolution/decay of the peaks is observable when $P_n(\lambda_{Bn}^1) > P_o(\lambda_{Bn}^1)$; where P_n is the power of the new peak and P_o is the power of the old peak at λ_{Bn}^1 , as shown in Fig. 5.

Fig. 6 shows the variation with temperature of the peak Bragg wavelength (λ_{Bn}^1 if $P_n(\lambda_{Bn}^1) > P_o(\lambda_{Bn}^1)$ or λ_B^1 otherwise). It can be seen that for $65^\circ\text{C} < T < 700^\circ\text{C}$, defined as the anomalous regime, a periodic discontinuity is seen, whereas for $700^\circ\text{C} < T < 900^\circ\text{C}$ there is a continuous monotonic increase. These discontinuities are due to the periodic growth and disappearance of the new and old peaks described above. Further, an overall temperature sensitivity of $12.673\text{pm}/^\circ\text{C}$ (regression fit) is obtained

until a complete erasure of the grating at $T=900^\circ\text{C}$. The present observation is very important from the viewpoint of thermal sensitivity of Bragg gratings and the application of FBGs as thermal sensors.

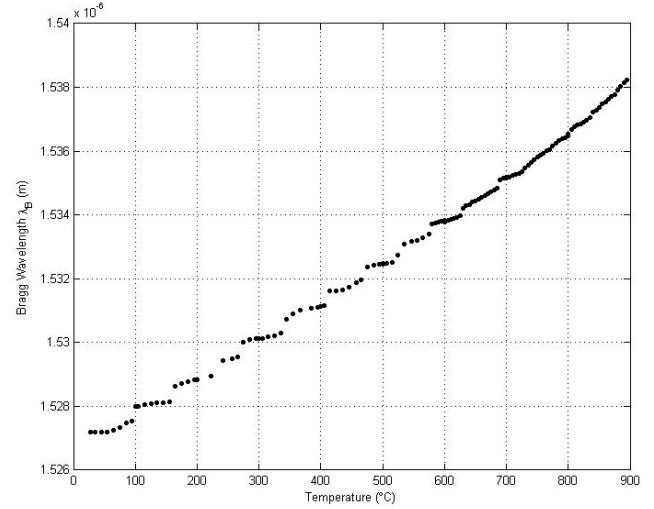


Fig. 6. Temperature sensitivity of the grating during erasure.

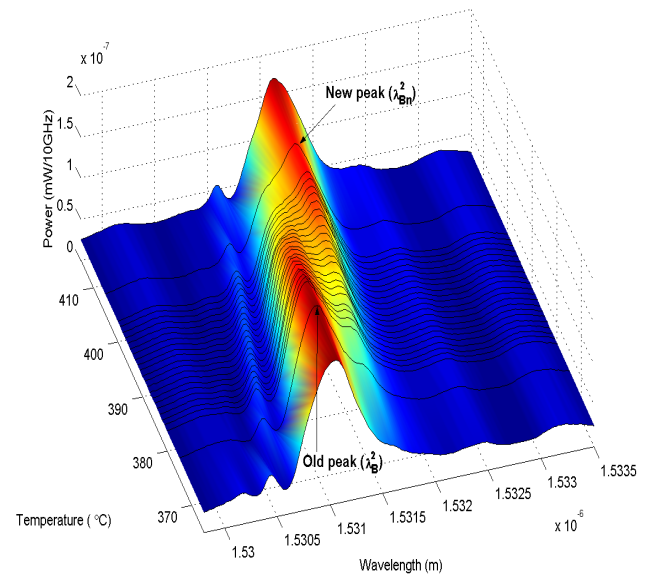


Fig. 7. Dynamics of the reflected spectrum for a boron co-doped germania fiber for a representative thermal window $375^\circ\text{C} < T < 415^\circ\text{C}$.

3.2. Boron co-doped Germania fiber

The experiment has been repeated on a grating inscribed in a Boron co-doped germania fiber (Newport) at $\lambda_B^2 = 1527.1\text{nm}$ using the same techniques described above and the data has been recorded at intervals of 1°C . Fig.7 shows the gradual formation of the new peak at λ_{Bn}^2 for $375^\circ\text{C} < T < 415^\circ\text{C}$, i.e. $P_n(\lambda_{Bn}^2) > P_o(\lambda_B^2)$. This shows that the observations are repeatable irrespective of the fiber type.

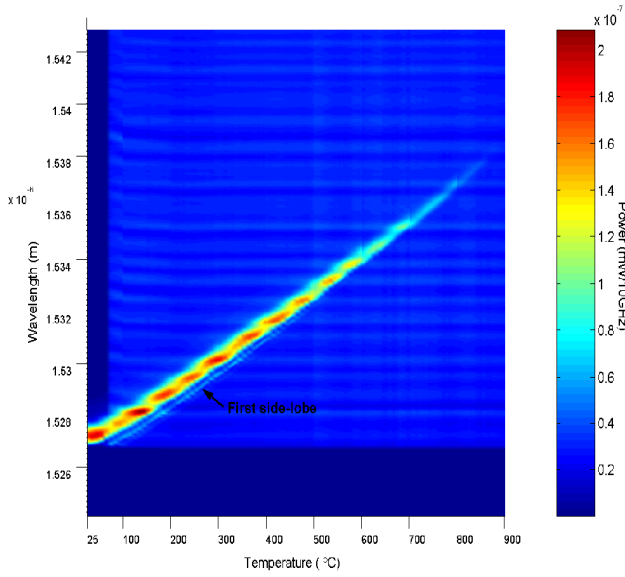


Fig. 8. Effect of temperature on Bragg peaks and first side-lobe.

3.3. First side-lobe

Fig. 8 shows the comparative thermal dynamics of the two Bragg resonance peaks and the first side-lobe (FSL). FSL at λ_{FSL} does not show any anomalous dynamics and maintains a monotonous slope irrespective of the anomaly occurring in the main-peak in the entire temperature of $65^\circ\text{C} < T < 700^\circ\text{C}$. These anomalies are observable using an analyzer with high resolution. Fig. 9 shows the variation of λ_{FSL} , λ_{B}^2 and λ_{Bn}^2 with T . Defining α_{Λ} and α_n as the thermal expansion and thermo-optic coefficient respectively, the dependence of the grating Bragg resonance on temperature given by the relation,

$$\Delta\lambda_{\text{B}} = \lambda_{\text{B}}(\alpha_{\Lambda} + \alpha_n)\Delta T \quad (1)$$

does not include the anomalous dynamics. It can be seen that during the growth,

$$\frac{d\lambda_{\text{FSL}}}{dT} (= 13.23\text{pm}/^\circ\text{C}) > \frac{d\lambda_{\text{B}}^2}{dT} (= 8.1\text{pm}/^\circ\text{C}) > \frac{d\lambda_{\text{Bn}}^2}{dT} (= 2.51\text{pm}/^\circ\text{C}) \quad (2)$$

Since $d\lambda_{\text{B}}^2/dT > d\lambda_{\text{Bn}}^2/dT$, at one particular temperature (T'), only one peak will be observed at λ'_{B} due to the merging of both λ_{B}^2 and λ_{Bn}^2 ; λ'_{B} will be repetitive with temperature (at different T') due to the periodic nature of the anomaly.

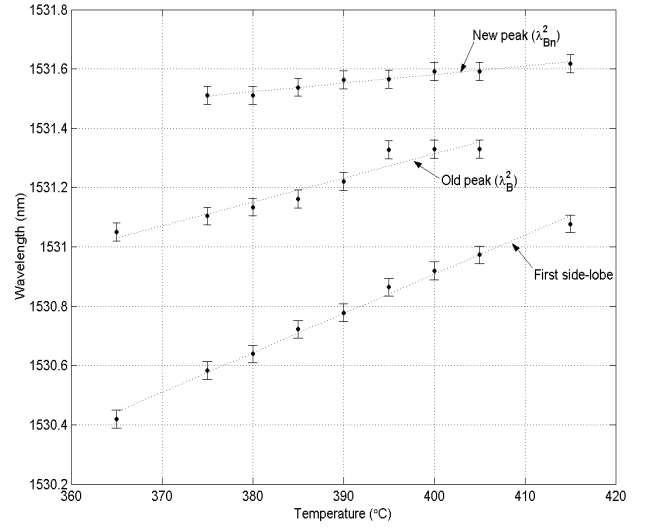


Fig. 9. Spectral shift of the reflection peaks as a function of temperature recorded in the anomalous regime.

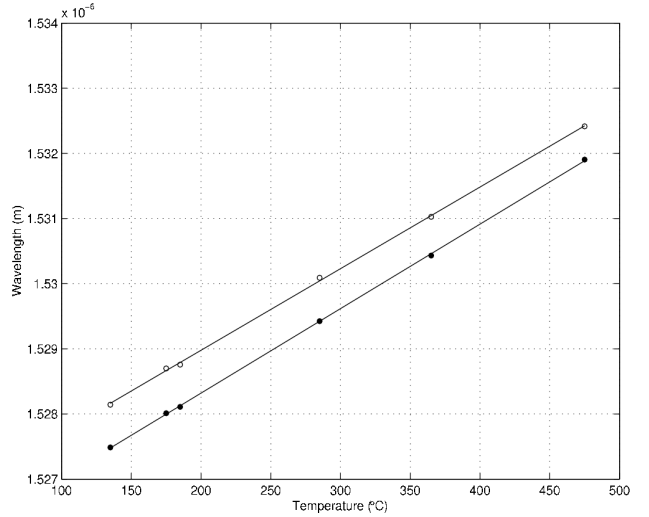


Fig. 10. Variation of first side lobe peak wavelength at λ'_{FSL} (●) and the Bragg wavelength at λ'_{B} (○) with temperature T' .

The variation of λ_{FSL} and λ'_{B} with T' is shown in Fig. 10. We see that,

$$\frac{d\lambda'_{\text{B}}}{dT'} (= 12.5\text{pm}/^\circ\text{C}) \approx \frac{d\lambda_{\text{FSL}}}{dT'} (= 12.9\text{pm}/^\circ\text{C}) \quad (3)$$

The conventional temperature sensitivity as defined by Eq. (1) holds good only for the temperatures T' . This result is also significant for sensing applications of FBGs.

3.4. Commercial gratings without side-lobes

The studies on thermal erasure dynamics have been undertaken on a commercial (Avensys Inc.) apodized

grating (without side lobes) having 99.99% reflectivity. Anomalous dynamics similar to that described in the previous sections is clearly visible in this grating also as shown in Fig. 11; the power transfer from old to new peak for the temperature range $100^\circ\text{C} < T < 200^\circ\text{C}$ is shown in Fig. 12. Presence of anomaly in gratings without side-lobes rules out any role played by κ_{dc} arising due to the non-uniform intensity profile on the observed anomalous behavior.

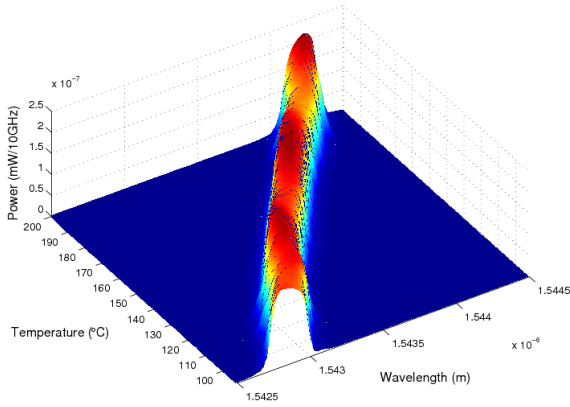


Fig. 11. Anomalous dynamics for a grating without side-lobes for $100^\circ\text{C} < T < 200^\circ\text{C}$.

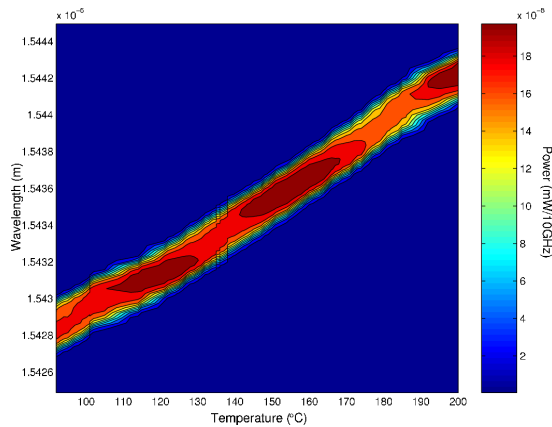


Fig. 12. Anomalous behavior of the grating with no side-lobes showing the power transfer from the old to new peak.

3.5. Influence of thermal stress

The effective refractive index n_{eff} of the fiber is dependent on the refractive index of both core and cladding. As the core and cladding materials are different ($\text{GeO}_2:\text{SiO}_2$ core and SiO_2 clad), there will be a mismatch in the thermal expansion at the core-cladding interface, which can induce a thermal stress on the core and result in the observed anomalous split in the peak depending on the stress.

To study the role of cladding, experiment was conducted without the cladding on the grating length. The grating region of the fiber was soaked in 40% HF for a duration of 55min and the etch process was controlled till the clad was completely removed. The non-clad grating

was placed in ICF and thermally ramped for $25^\circ\text{C} < T < 110^\circ\text{C}$. The presence of anomaly as shown in Fig. 13, excludes the role of thermal stress arising from core-clad mismatch, on the anomaly observed.

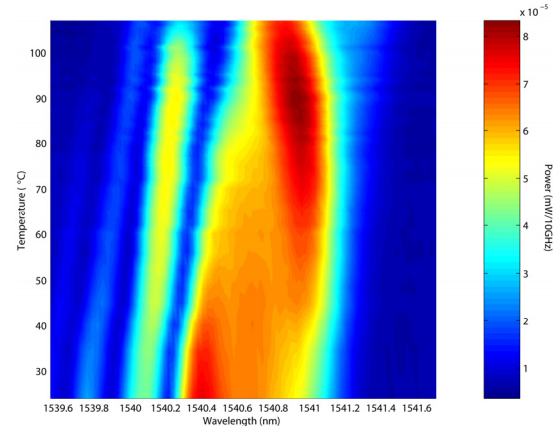


Fig. 13. Anomalous thermal behavior of non-clad grating for $24^\circ\text{C} < T < 107^\circ\text{C}$ showing the transfer of power from the old peak (λ_B) to the new peak (λ_{Bn}) and the unaffected profile of first side-lobe λ_{FSL} .

3.6. Coefficient kinetics

As given in Eq. (1), change in temperature T affects the pitch Λ of the grating and the effective index n_{eff} of the material & the sensitivity of a grating written in a germanium doped silica fiber is dependent on the thermal-expansion coefficient α_Λ & thermo-optic coefficient α_n . The typical values of α_Λ and α_n are $0.55 \cdot 10^{-6}/^\circ\text{C}$ and $8.6 \cdot 10^{-6}/^\circ\text{C}$ respectively. Thus, the main contribution to the shift in the Bragg resonance due to temperature is due to α_n of the fiber core material. Since the difference in the temporal kinetics of the coefficients, $d\alpha_n/dt \neq d\alpha_\Lambda/dt$, can also cause the observed anomaly, an experiment was conducted where the grating was annealed for 16hrs at $T=92^\circ\text{C}$ where $P_0(\lambda_B) \approx P_n(\lambda_{Bn})$. A deterioration in the reflectivity was observed with a proportional drop in P_0 and P_n as shown in Fig.14, eliminating the possibility of relative temporal kinetics of the coefficients.

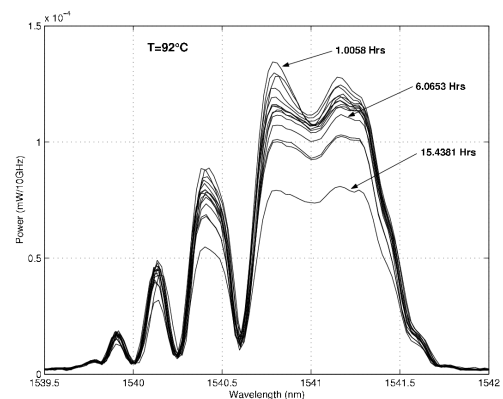


Fig. 14. Reflection spectrum of FBG during ~16 hrs annealing at $T=92^\circ\text{C}$.

3.7. Heating/Cooling cycles

If the observed anomaly is due to the distortion in the refractive index profile of the grating, heating and subsequently cooling of the grating should show a reversible effect, provided the maximum temperature does not cross the glass transition temperature (T_g) of the core material. Heating and cooling of a grating for $25^\circ\text{C} < T < 170^\circ\text{C}$, at three different rates were performed as shown in Fig.15. Inset in Fig.15 shows the power variation with temperature due to the cyclic formation of the new peaks and the decay of the old peaks during the third heating/cooling cycle. The periodicity of the anomaly is found to increase with each consecutive cycle indicating an irreversible change in the average refractive index of the grating.

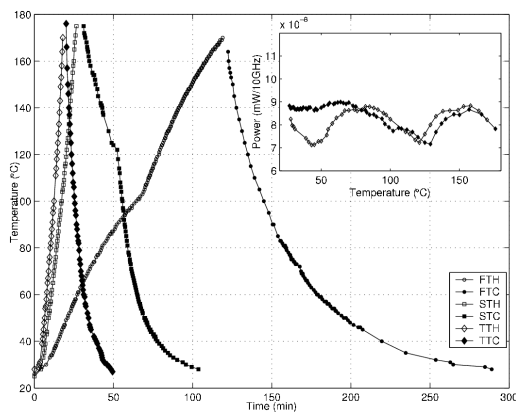


Fig. 15. Three heating and cooling rates. (F: First, S: Second, T: Third, TH: Thermal Heating and TC: Thermal Cooling.)

The anomalous phenomenon followed an identical reverse behavior during the cooling cycle, as shown in the inset of Fig. 15 for Third Thermal Heating (TTH) /Third Thermal Cooling (TTC). That is, during cooling the power of the new peak at λ_{Bn}^1 is reduced with the simultaneous growth of the old-peak at λ_B^1 as shown in Fig.16 for $80^\circ\text{C} < T < 160^\circ\text{C}$.

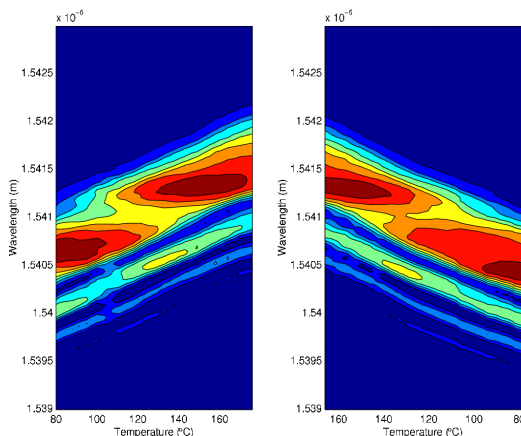


Fig. 16. The reversible power transfer between the old and new peaks during heating and cooling.

4. Analysis of anomaly

The observed temperature induced distortion in refractive index modulation profile can be understood in the light of compaction-densification model [13]. Hidayat *et al* [14] have suggested that the structural change resulting from the inscription of Type I gratings in non-hydrogenated $\text{GeO}_2:\text{SiO}_2$ fibers produces a change in the thermal expansion coefficient. According to their hypothesis, exposure to an interference fringe pattern manifests as a modulation of the thermal expansion coefficient along the fiber axis. We propose that during the fabrication process of a grating, the modulation in the thermal expansion coefficient brought about by the interference fringes results in a non-uniform expansion throughout the grating length which in turn results in the distortion of the refractive index profile with increase/decrease in temperature. Since the reflection spectrum of a grating can be approximated as the Fourier transform of the refractive index profile, any distortion in the index profile results in the observed anomalous behavior in the reflection spectrum.

It is interesting to note here that nano-indentation studies on the exposed and unexposed regions of the photosensitive glass, undertaken recently by the authors [15] have revealed a substantial change in the Young's modulus. This observation indicates the possibility of local structural change in the exposed region and the associated changes in mechanical and other properties of the glass. Rigorous experimental investigations involving study of changes in the local structure and other properties of the glass due to UV exposure are underway. These studies are expected to throw more light on the observed phenomenon.

5. Conclusions

In this paper, we report an anomalous growth of a new peak in the Bragg reflection spectra during the thermal erasure process. The new peak occurs on the longer wavelength side of the spectrum during heating and on the shorter wavelength side during cooling, following an identical reverse dynamics. A commercial grating with 99.9% reflectivity has also been found to exhibit a similar decay dynamics. Also, it is shown that the side-lobe dynamics does not mimic the anomaly of the main Bragg resonance peak.

Detailed experiments undertaken in this study indicate that the observed anomalous behavior is due to the distortion of the refractive index modulation profile.

The present study is important not only from the viewpoint of understanding the thermal behavior of FBG, but also important from the application point of view.

References

- [1] K. O. Hill, Y. Jujii, D. C. Johnson, B. S. Kawasaki, *Appl. Phys. Lett.* **32**, 647 (1978).
- [2] K. O. Hill, Gerald Meltz, *J. Lightwave Technol.*

- 15**(8), 1263 (1997).
- [3] C. R. Giles, *J. Lightwave Technol.* **15**(8), 1391 (1997).
- [4] A. D. Kersey, M. A. Davis, H. J. Patrick, M. LeBlanc, K. P. Koo, C. G. Askins, M. A. Putnam, E. Joseph Friebele, *J. Lightwave Technol.*, **15**(8), 1442 (1997).
- [5] T. Erdogan, V. Mizrahi, P. J. Lemaire, D. Monroe, *J. Appl. Phys.* **76**(1), 73 (1994).
- [6] B. Pommellec, P. Niay, P. Bernage, M. Douay, J. F. Bayon, V.B. Soulimov, Proc. COST 246 European Workshop on Bragg Grating Reliability, 177 (1995).
- [7] H. Patrick, S. L. Gilbert, A. Lidgard, M. D. Gallagher, *J. Appl. Phys.* **78**(5), 2940 (1995).
- [8] D. L. Williams, R. P. Smith, *Electron. Lett.* **31**(24), 2120 (1995).
- [9] R. J. Egan, H. G. Inglis, P. Hill, P. A. Krug, F. Ouellette, Proc. OFC'96, 83 (1996).
- [10] S. Kannan, P. J. Lemaire, Proc. OFC'96, 84 (1996).
- [11] I. Riant, S. Borne, P. Sansonetti, Proc. OFC'96, 86 (1996).
- [12] S. R. Baker, H. N. Rourke, V. Baker, D. Goodchild, *J. Lightwave Technol.* **15**(8), 1470 (1997).
- [13] J. P. Bernardin, N. M. Lawandy, *Opt. Commun.* **79**, 194 (1990).
- [14] A. Hidayat, Q. Wang, P. Niay, M. Douay, B. Pommellec, F. Kherbouche, I. Riant, *Appl. Optics* **40**, 2632 (2001).
- [15] A. Rahman, U. Ramamurty, S. Asokan, Nanoindentation studies on photosensitive glass performs, to be published.

*Corresponding author: aashia.rahman@gmail.com